

Potential Anti-infective Targets in Pathogenic Yeasts: Structure and Properties of 3,4-Dihydroxy-2-butanone 4-phosphate Synthase of *Candida albicans*

Stefanie Echt¹†, Stefanie Bauer²†, Stefan Steinbacher², Robert Huber²
Adelbert Bacher¹ and Markus Fischer¹*

¹Lehrstuhl für Organische Chemie und Biochemie Technische Universität München, Lichtenbergstr. 4 D-85747 Garching, Germany

²Max-Planck-Institut für Biochemie, Abteilung für Strukturforschung, Am Klopferspitz 18a, D-82512 Martinsried, Germany

A synthetic gene specifying a putative 3,4-dihydroxy-2-butanone 4-phosphate synthase of *Candida albicans* directed the synthesis of a 22.5 kDa peptide in a recombinant *Escherichia coli* strain. The recombinant protein was purified to apparent homogeneity by two chromatographic steps and was shown to catalyze the formation of L-3,4-dihydroxy-2-butanone 4-phosphate from ribulose 5-phosphate at a rate of 332 nmol mg⁻¹ min⁻¹. Hydrodynamic studies indicated a native molecular mass of 41 kDa in line with a homodimer structure. The protein was crystallized in its apoform. Soaking yielded crystals in complex with the substrate ribulose 5-phosphate. The structures were solved at resolutions of 1.6 and 1.7 Å, respectively, using 3,4-dihydroxy-2-butanone 4-phosphate synthase of *E. coli* for molecular replacement. Structural comparison with the orthologs of *Magnaporthe grisea* and *Methanococcus jannaschii* revealed a hitherto unknown conformation of the essential acidic active-site loop.

© 2004 Elsevier Ltd. All rights reserved.

Keywords: *Candida albicans*; riboflavin biosynthesis; 3,4-dihydroxy-2-butanone 4-phosphate synthase; crystal structure; synthetic gene

*Corresponding author

Introduction

Flavocoenzymes are essential cofactors for catalysis of a wide variety of redox reactions.¹ Moreover, they are involved in numerous other physiological processes involving light sensing,^{2,3} bioluminescence,^{4–6} circadian time-keeping and DNA repair.⁷

The universal precursor of flavocoenzymes, vitamin B₂ (riboflavin), is biosynthesized by plants and many microorganisms but must be obtained from dietary sources by animals. The biosynthesis of the vitamin has been studied in considerable detail in eubacteria and fungi (Figure 1).^{8–10} The pyrimidine moiety and the ribityl side chain are

both derived from GTP (1) which is converted to 5-amino-6-ribitylamino-2,4(1H,3H)-pyrimidinedione 5-phosphate by a series of three enzyme-catalyzed reactions.^{11–16} The dephosphorylation of this intermediate by a hitherto unknown enzyme affords 5-amino-6-ribitylamino-2,4(1H,3H)-pyrimidinedione (2) which serves as substrate for 6,7-dimethyl-8-ribityllumazine synthase. The second substrate of that enzyme is synthesized from ribulose 5-phosphate (3) by 3,4-dihydroxy-2-butanone 4-phosphate synthase. Compounds 2 and 4 are condensed by 6,7-dimethyl-8-ribityllumazine synthase.^{17–19} The lumazine derivative 5 subsequently undergoes a dismutation affording riboflavin (6) and the biosynthetic intermediate 2 which is recycled in the pathway.^{20–23} In summary, the formation of one equivalent of riboflavin requires one equivalent of compound 1 and two equivalents of compound 3.

The reaction catalyzed by 3,4-dihydroxy-2-butanone 4-phosphate synthase involves a skeletal rearrangement conducive to the release of carbon atom 4 of the substrate, ribulose 5-phosphate, as formate (Figure 2). Moreover, the position 1 hydroxyl group of the substrate is removed. The hypothetical reaction mechanism suggests a crucial role for acid/base catalysis, and polar ligands are

† S.E. and S.B. contributed equally to the paper.

Present address: S. Steinbacher, Division of Chemistry and Chemical Engineering, Mail Code 114-96, California Institute of Technology, Pasadena, CA 91125, USA.

Abbreviations used: CA, *Candida albicans*; CD, circular dichroism; DHBP, L-3,4-dihydroxy-2-butanone 4-phosphate; DHBPS, 3,4-dihydroxy-2-butanone 4-phosphate synthase; r.m.s.d., root mean square deviation; Ru5P, ribulose 5-phosphate.

E-mail address of the corresponding author: markus.fischer@ch.tum.de

amplified from genomic DNA by PCR and ligated into pNCO113. DNA-sequencing revealed five single-base substitutions (Table 1) conducive to one amino acid exchange (Q183R) by comparison with the reported open reading frame orf6.2440.

Plasmids carrying the wild-type or synthetic *C. albicans* gene under the control of a T5 promoter and *lac* operator directed the synthesis of a 22.5 kDa protein in recombinant *E. coli* strains. Enzyme assays of crude cell extract afforded dihydroxy-2-

Table 1. Nucleotide and amino acid exchanges of pNCO-CARib3-WT as compared to orf6.2440

| Base number | orf6.2440 | pNCO-CARib3-WT | Amino acid exchange |
|-------------|-----------|----------------|---------------------|
| 414 | C | T | - |
| 426 | G | A | - |
| 477 | A | T | - |
| 480 | T | A | - |
| 581 | A | G | Q181R |

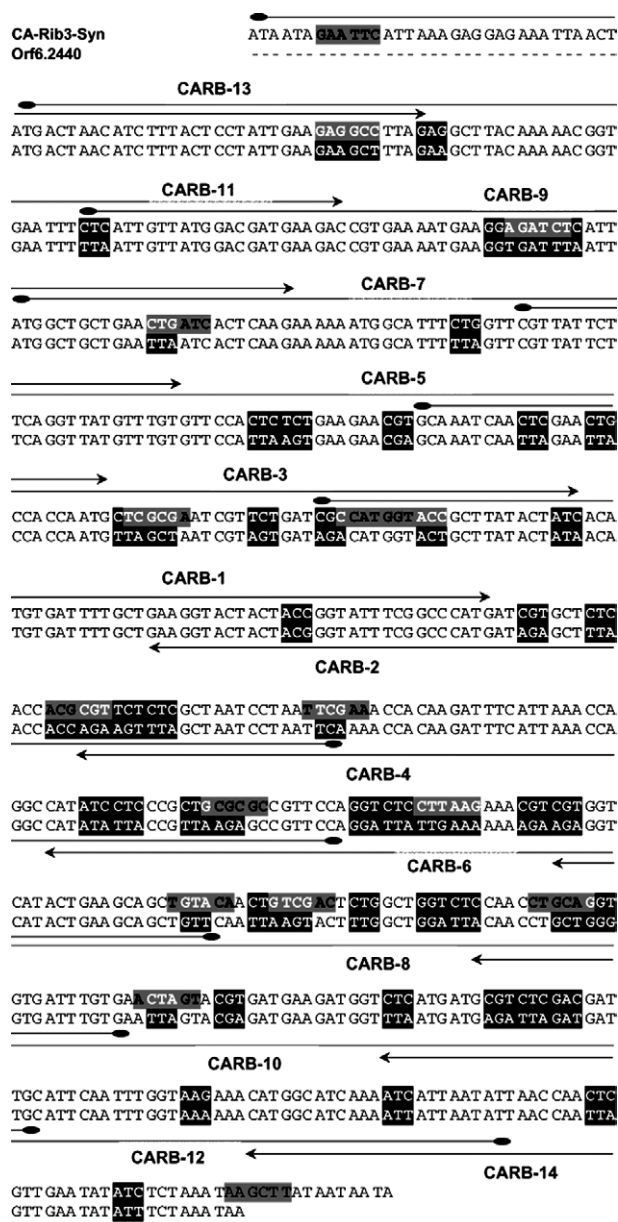


Figure 3. Synthesis of the 3,4-dihydroxy-2-butanone 4-phosphate synthase gene of *C. albicans* with optimized codon usage for *E. coli*. Alignment of the wild-type DNA sequence (orf6.2440) and the synthetic DNA sequence (CA-Rib3-syn) with 5' and 3' overhangs including the synthetic EcoRI and HindIII sites. Changed codons are shaded in black. New single restriction sites are shaded in grey. Oligonucleotides used as forward primers are drawn above and reverse primers below the aligned DNA sequences.

butanone 4-phosphate synthase activities of 70 nmol min⁻¹ mg⁻¹ and 21 nmol min⁻¹ mg⁻¹ for XL1 strains carrying the plasmids pNCO-CARib3-syn (synthetic gene) and pNCO-CARib3-WT (wild-type gene), respectively. This reflects an approximately three times higher expression level of the optimised gene sequence as judged by SDS-PAGE (not shown).

The recombinant protein was purified to apparent homogeneity by two chromatographic steps. Electrospray mass spectrometry afforded a peak corresponding to a molecular mass of 22,530 indicating cleavage of the initial methionine (calculated mass of the full length protein, 22,658; calculated mass without initial methionine, 22,527). Edman degradation of the N terminus afforded the sequence TNIFTPI. Analogous observations were made with the purified mutant CARib3-proteins.

Analytical ultracentrifugation

The wild-type enzyme sediments as a single, symmetrical boundary with a velocity of 3.0 S (20 °C). Sedimentation equilibrium centrifugation afforded a relative mass of 41 kDa (Figure 4) indicating a homodimer structure in analogy with the homodimeric enzymes of *E. coli*,^{31,32} *M. jannaschii*^{25,33} and *M. grisea*.³⁰

Kinetic characterization

The purified wild-type enzyme catalyzes the conversion of ribulose 5-phosphate into 3,4-dihydroxy-2-butanone 4-phosphate at a rate of $v_{\max} = 332 \text{ nmol min}^{-1} \text{ mg}^{-1}$ with an apparent K_M of 37 μM (Table 2). The corresponding v_{\max} -values of the *M. jannaschii* and *M. grisea* orthologs are 174³³ and 112 nmol min⁻¹ mg⁻¹,³⁴ respectively. Since both enantiomers of 3,4-dihydroxy-2-butanone 4-phosphate can serve as substrates for 6,7-dimethyl-8-ribityllumazine synthase,¹⁹ we determined the configuration of the product of *C. albicans* 3,4-dihydroxy-2-butanone 4-phosphate synthase. The CD-spectrum shown in Figure 5 is that expected for the L-isomer.²⁴

Sequence alignments and comparison of the X-ray structures of *M. grisea* and *M. jannaschii* DHBPS revealed a slightly different active site architecture between the two orthologs.²⁵ Based on this finding, the mutants CARib3-C59A, CARib3-Y87A, CARib3-D92A and CARib3-E166A

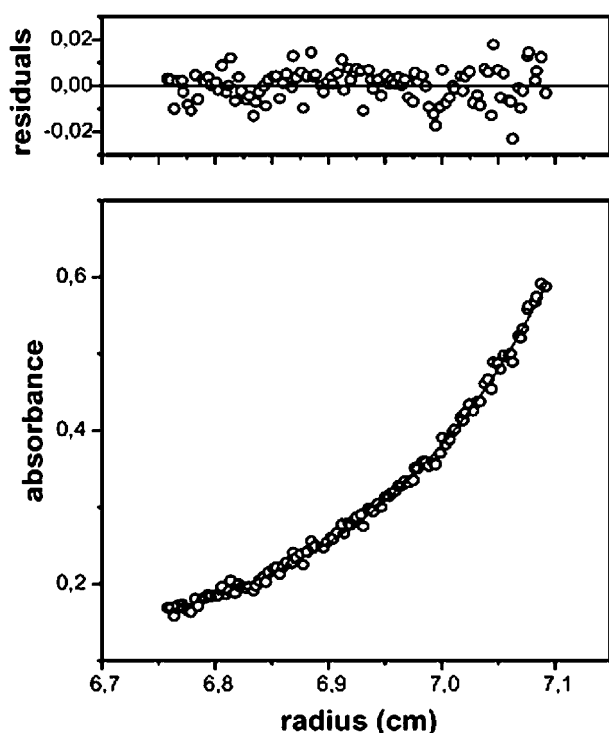


Figure 4. Sedimentation equilibrium centrifugation of 3,4-dihydroxy-2-butanone 4-phosphate synthase of *C. albicans*.

were constructed, purified and kinetically characterized for further characterization of the active site (Table 2, Figure 6). The residues C59 and E166 are equivalent to residues C55 and E185 of *M. jannaschii* 3,4-dihydroxy-2-butanone 4-phosphate synthase, which have already been studied by site-directed mutagenesis.³³ Presumably, the strictly conserved glutamate initiates catalysis by abstracting the proton of carbon atom 3, thus affording enediol 7 (Figure 2). CARib3-E166A, as the corresponding E185-mutants, does not show any residual activity, which emphasizes the essential role of this residue.

C55 in *M. jannaschii* was proposed to act as a proton relais during dehydration of carbon atom 1 in concert with the nearby H147. Exchange of C55 by serine or glycine results in mutants with considerable residual activity (44%, 19%, respectively) and increased K_M -values. CARib3-C59A displays a residual activity of 70% and a K_M -value of 536 μM compared to 37 μM of the wild-type. This

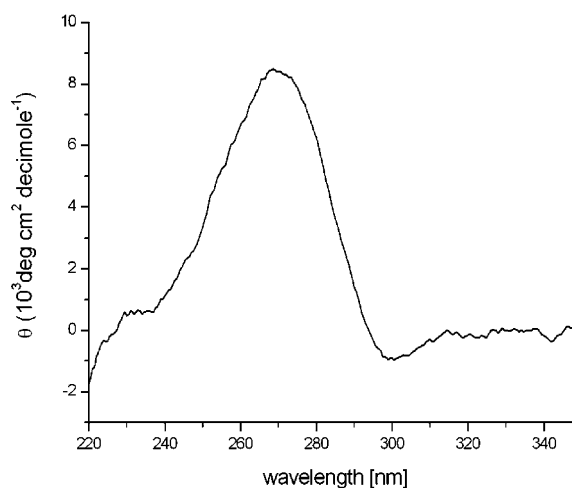


Figure 5. CD-Spectrum of 3,4-dihydroxy-2-butanone 4-phosphate enzymatically formed by 3,4-dihydroxy-2-butanone 4-phosphate synthase of *C. albicans*.

rather accounts for a geometrical role of the cysteine residue.

H147 is hydrogen bonded to N106 whereas in the *M. grisea* enzyme the corresponding H136 forms a dyad with D99. Generally, the strictly conserved histidine interacts with an asparagine in archaea, whereas in eubacteria, yeasts and plants either an aspartate or glutamate takes this place (Figure 6). In *C. albicans*, the corresponding residue is D92. Replacement of H147 in *M. jannaschii* by serine results in 12% residual activity.³³ CARib3-D92A is completely inactive and, additionally, seems to be destabilized in its overall structure, since expression at 37 °C resulted in insoluble protein. This problem could be overcome by lowering the expression temperature to 20 °C using the inducible *E. coli* strain M15 [pRep4] for expression. The high residual activity of CARib3-C59A taken together with the obvious indispensability of a functional H136-D92 dyad suggests that the histidine acts as the actual proton relais during the formation of enediol 9 (Figure 2).

Besides D92, Y87 is another active site residue, which is not strictly conserved among DHBPS orthologs. In the *M. grisea* enzyme, the corresponding Y94 was found to form an H-bond to the substrate's C2 carbonyl oxygen, but since this residue can be replaced by phenylalanine (F101 in *M. jannaschii* DHBPS), this interaction was

Table 2. Steady state kinetic analysis of wild-type and mutant DHBPS of *C. albicans*

| Enzyme | v_{\max} (nmol mg ⁻¹ min ⁻¹) | Percentage of wild-type activity (%) | K_M (μM) | Accession no. |
|-----------|--|---|-------------------------|---------------|
| Wild-type | 332 | 100 | 37 | AY504626 |
| C59A | 232 | 70 | 536 | AY549492 |
| Y87A | 7 | 2 | 117 | AY549495 |
| D92A | – | – | – | AY549494 |
| E166A | – | – | – | AY549493 |

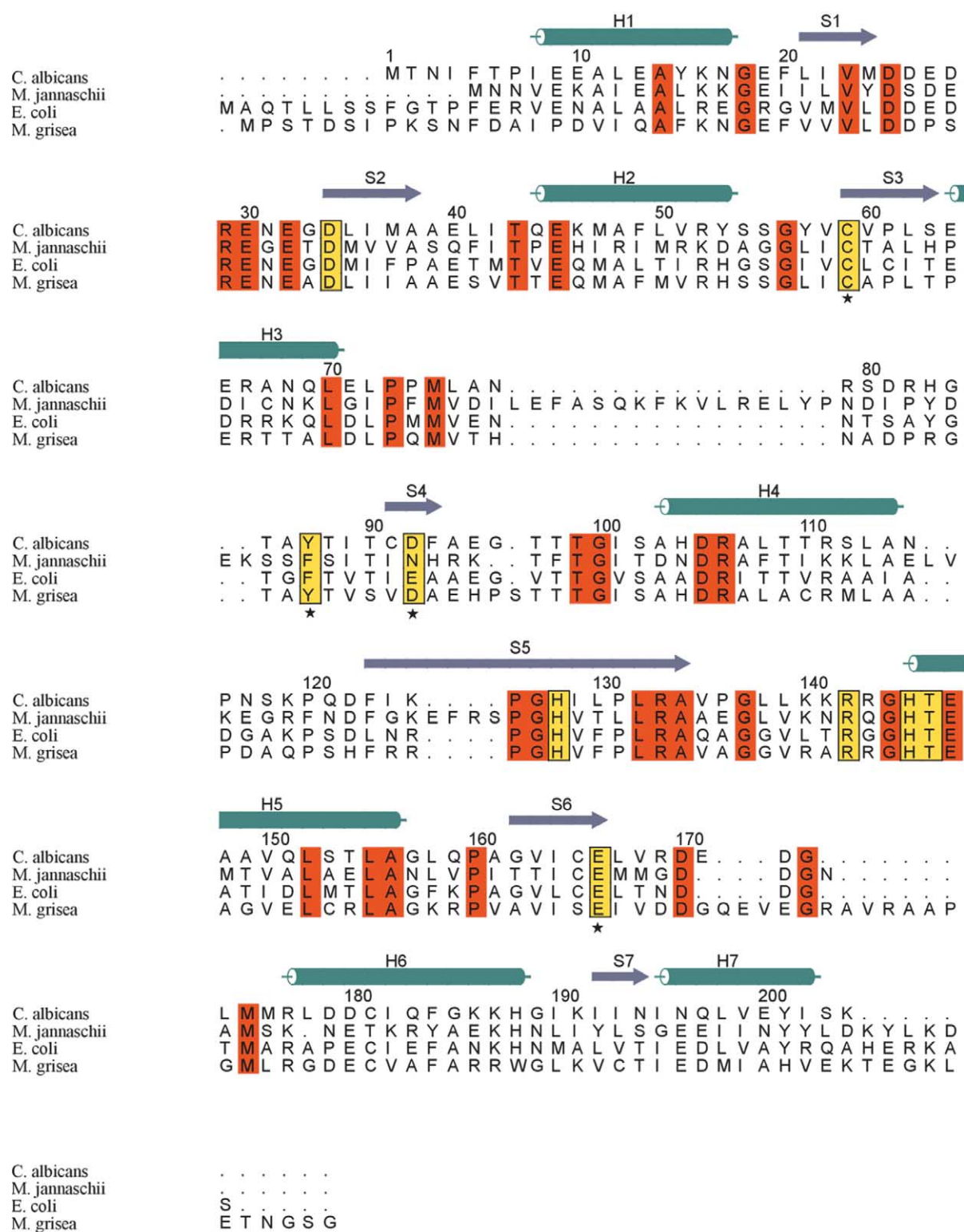


Figure 6. Sequence alignment of 3,4-dihydroxy-2-butanone 4-phosphate synthases with known X-ray structure. Residues mutated in this study are marked with stars. Conserved residues are marked red. Active site residues are marked yellow. Secondary structure elements of the *C. albicans* enzyme are shown above the alignment.

supposed to be non-essential. Nevertheless, since CARib3-Y87A shows only 2% residual activity, the presence of the aromatic residue is obviously important, possibly for shielding the reaction intermediates from water.

Crystal structure determination

The crystals of DHBPS of *C. albicans* belonged to space group *P1* (Table 3; cell constants: $a=40.439$ Å, $b=48.134$ Å, $c=59.804$ Å, $\alpha=66.229^\circ$, $\beta=71.979^\circ$,

$\gamma = 89.856^\circ$). The structure was solved by molecular replacement using the model of *E. coli* DHBPS (PDB-ID: 1G57) as Patterson search model in the absence of ligands. The asymmetric unit contained one dimer, which reflects the solution state of the enzyme. The model was refined at 1.6 Å to an *R*-factor of 19.2% and an *R*_{free} of 21.9%. The final model contains 390 residues out of 406. No electron density is present for residues 78–83 and the first two N-terminal residues.

Co-crystallization of the enzyme with EDTA afforded crystals of the same space group with one dimer in the asymmetric unit. Soaking these crystals with 2 mM D-ribulose 5-phosphate clearly displayed the bound D-ribulose 5-phosphate. The structure of the Ru5P-complex was solved by molecular replacement and refined at a resolution of 1.7 Å. The final model of the complex consists of 392 amino acid residues with an *R*-factor of 18.4% and an *R*_{free} of 21.8%. Soaking the EDTA co-crystals with MgCl₂ and D-ribulose 5-phosphate failed because crystals cracked even with low concentrations of substrates.

Although refined without non-crystallographic symmetry restraints, the monomers of the ligand-free enzyme and of the complex were very similar, respectively, showing r.m.s. deviations of only 0.28 Å for 195 C^α-atoms (ligand-free) and 0.22 Å for 196 C^α-atoms (Ru5P-complex).

Overall three-dimensional architecture

In accordance with the structures of the enzymes of *E. coli*, *M. grisea* and *M. jannaschii*, the DHBPS of *C. albicans* is an $\alpha + \beta$ homodimeric protein of 46 kDa. Each monomer consists of seven helices surrounding the central eight-stranded mixed β sheet which is twisted nearly 180° from end to end.

The N and C termini of each monomer are located on the far ends of the dimer. The connectivity of the mixed β sheet is complex and rather unusual. It contains three crossovers connecting the C-terminal end of $\beta 2$ to the N-terminal end of $\beta 3$, the C-terminal end of $\beta 3$ to the N-terminal end of $\beta 4$, and the C-terminal end of $\beta 7$ to the N-terminal end of $\beta 8$. Each of the crossovers has a single α helix of two to three turns, which are located on the same side of the β sheet. Between the C-terminal end of $\beta 4$ and the N-terminal end of $\beta 5$ there is a region of six residues, which are not defined by the electron density. The major interactions between the two monomers in the dimer interface are hydrophobic. Figure 7 shows a ribbon presentation of the DHBPS dimer with bound ribulose 5-phosphate.

In contrast to the three other known DHBPS structures, the active site acidic loop (Glu32, Asp34, Glu166) of the *C. albicans* enzyme is well defined in the electron density in the ligand-free structure as well as in the Ru5P-complex while the loop around residues 78–83 which corresponds to the insertion around Tyr95 in the *M. jannaschii* structure is fully disordered.

The *C. albicans* monomer can be superimposed with r.m.s. deviations of 0.86 Å (*M. grisea*), 1.22 Å (*M. jannaschii*) and 1.03 Å (*E. coli*) for 188 (*M. grisea*), 168 (*M. jannaschii*) and 186 (*E. coli*) C^α-atoms reflecting a high similarity.

Active site architecture

The two topologically equivalent active sites of the *C. albicans* enzyme, as defined by the location of the bound D-ribulose 5-phosphate, are located at the dimer interface. The surface of each active site cavity is mainly formed by one respective monomer, and is lined by the central β -sheet and

Table 3. X-ray data processing and refinement statistics

| | Native | Ru5P-complex |
|--|--|--|
| Cell constants | $a = 40.4 \text{ \AA}, b = 48.1 \text{ \AA}, c = 59.8 \text{ \AA}$ $\alpha = 66.2^\circ, \beta = 71.9^\circ, \gamma = 89.8^\circ$ | $a = 40.2 \text{ \AA}, b = 47.9 \text{ \AA}, c = 59.8 \text{ \AA}$ $\alpha = 66.4^\circ, \beta = 72.3^\circ, \gamma = 89.9^\circ$ |
| Space group | P1 | P1 |
| Resolution (Å) overall (last shell) | 20–1.6 (1.66–1.6) | 20–1.66 (1.672–1.66) |
| Reflections, unique | 43,264 | 39,461 |
| Multiplicity | 3.8 | 3.2 |
| <i>R</i> _{merge} ^a overall (last shell) | 0.059 (0.221) | 0.032 (0.174) |
| Completeness (%) overall (last shell) | 84.4 (81.9) | 77.3 (28.7) |
| <i>I</i> / σ | 27.7 | 22.2 |
| Solvent molecules | 692 | 672 |
| Non hydrogen ligand atoms | – | 27 |
| <i>R</i> _{cryst} ^b (%) overall (<i>R</i> _{free} ^c) | 19.2 (21.9) | 18.4 (21.8) |
| R.m.s.d. bond lengths (Å) | 0.005 | 0.005 |
| R.m.s.d. bond angles (°) | 1.19 | 1.27 |
| Average <i>B</i> -value (Å ²) protein | 12.9 | 12.1 |
| Average <i>B</i> -value (Å ²) ligand | – | 27.8 |
| Average <i>B</i> -value (Å ²) solvent | 28.3 | 28.0 |
| Φ, Ψ angle distribution for residues ^c | | |
| In most favoured regions (%) | 88.9 | 89.9 |
| In additional allowed regions (%) | 11.1 | 10.1 |

^a $R_{\text{merge}} = \sum_{hkl} [(\sum_i |I_i - \langle I \rangle|) / \sum_i I_i]$.

^b $R_{\text{cryst}} = \sum_{hkl} ||F_{\text{obs}}| - |F_{\text{calc}}|| / \sum |F_{\text{obs}}|$.

^c *R*_{free} is the cross-validation *R*-factor computed for the test set of 5% of unique reflections.

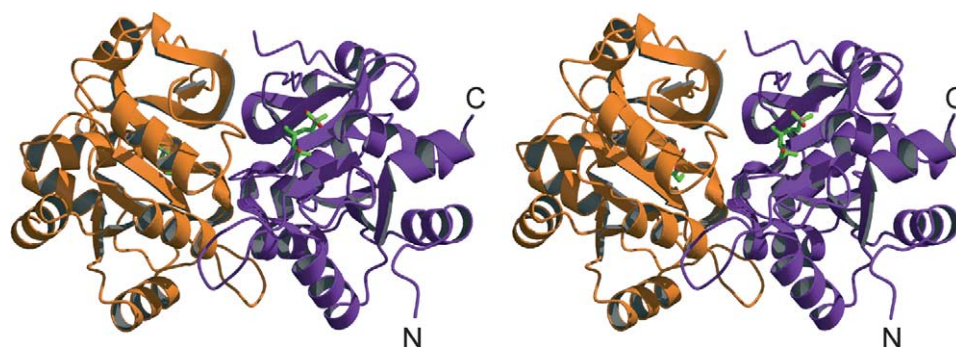


Figure 7. Stereoview of the dimeric 3,4-dihydroxy-2-butanone 4-phosphate synthase of *C. albicans*. Subunits are shown in orange and purple, respectively. Bound ribulose 5-phosphate is shown in light green.

the N terminus of the α -helix from Arg142 to Thr146 which contributes His145 as central active site residue. The acidic active site loop from Glu30 to Asp34 and Glu166 as well as loop structures around Tyr87, Thr99 and His128 constitute the other parts of the active site. Most of these residues reside within one monomer with the exception of the loops around Thr99 and His128, which belong to the neighboring monomer. **Figure 8** shows the ribulose 5-phosphate binding site from *C. albicans* DHBPS with the final $2F_{\text{obs}} - F_{\text{calc}}$ electron density map covering the bound molecule. The phosphate group of the ligand is hydrogen bonded to the side-chains of Thr85, Arg142, His145 and Thr146. The stabilization of the C1-C2 part is performed by Asp34 of the acidic cluster which is hydrogen bonded to the C2 carbonyl oxygen. The C3 hydroxyl group is fixed by hydrogen interactions between Glu166 and Cys59 while the C4 hydroxyl group stabilization is performed by a hydrogen bond to the hydroxyl group of Tyr87. All interactions are performed between the ligand and the side-chains of these conserved amino acid residues.

Due to the absence of divalent metal ions, the ribulose group of the ligand shows a completely

different binding mode in comparison with the modeled *M. grisea* complex (data not shown) and the experimental complex of mutant (H147S) *M. jannaschii* DHBPS (**Figure 9**). In these structures, the cysteine residue is hydrogen bonded to the C1 hydroxyl group, the aspartate forms a hydrogen bond to the C4 hydroxyl group and the histidine residue which is exchanged against a serine in *M. jannaschii* does not interact with the ligand at all instead of a further interaction to the C1 hydroxyl group. His145, stabilizing the Zn^{2+} in the *M. jannaschii* DHBPS, forms a hydrogen bond to one of the phosphate oxygen atoms. Tyr87 corresponding to Tyr94 in *M. grisea* interacts with the C2 carbonyl oxygen while in *M. jannaschii*, this residue corresponds to a phenylalanine, thus only contributing hydrophobic interactions. Only the glutamate shows the same interaction as in the other two complexes as well as the binding mode for the phosphate group. A major contribution to the binding affinity of the substrate Ru5P can be seen in the interactions of its phosphate group with the well defined phosphate binding site. Therefore, it is not surprising that the substrate can also be bound to the active site in the absence of metal ions. The

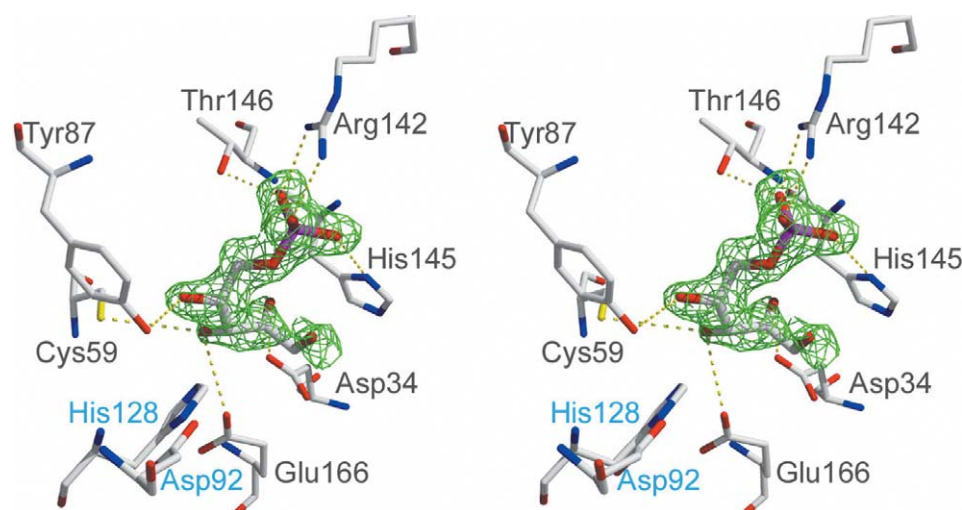


Figure 8. Stereoview of the active site of 3,4-dihydroxy-2-butanone 4-phosphate synthase of *C. albicans* with bound ribulose 5-phosphate. The final $2F_{\text{o}} - F_{\text{c}}$ electron density map covering the ligand is contoured at 1.0σ . Residues marked in blue are from the neighboring subunit.

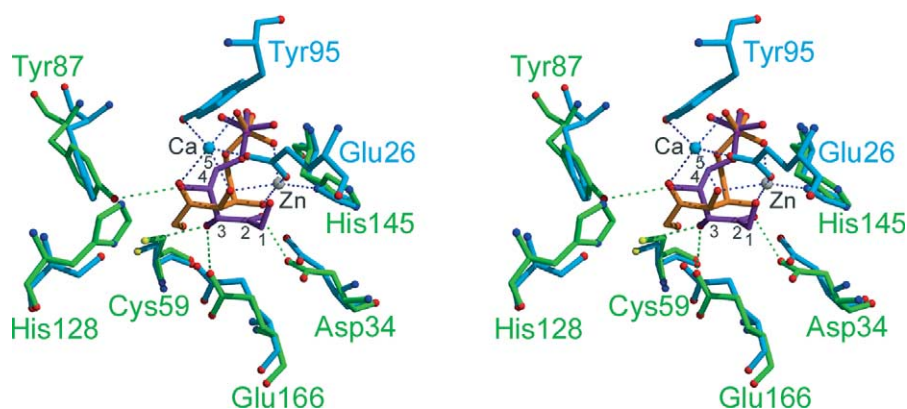


Figure 9. Comparison of the *C. albicans* DHBPS (green) active site to that of *M. jannaschii* (blue): superposition of the active sites shows two different conformations for bound Ru5P (*C. albicans*, purple; *M. jannaschii*, orange). For *M. jannaschii* DHBPS interactions with the bound metal ions are shown (Ca, blue; Zn, grey).

relatively high temperature factor for the bound Ru5P (27.8 \AA^2) in comparison to the average *B*-factor of the protein model (12.1 \AA^2) suggests a weak binding affinity for the ligand in this non-physiological extended conformation. Furthermore the C1/C2-part of the ligand seems to be rather flexible in comparison with the phosphate group and the C3/C4-groups which were well defined by the electron density (Figure 8). When bound to metal ions at the active site of *M. jannaschii* DHBPS Ru5P is found in a compact geometry in which the C5 atom can migrate to the C3 atom and ultimately release the C4 atom as formate.

Figure 10 shows a comparison of the *C. albicans* ribulose 5-phosphate complex and the complexes of *M. jannaschii* (blue) and *M. grisea* (green) in respect of the conformations of the acidic loop (flap I) and the loop around residues 78–83 (flap II). Superposition of the native enzyme and the ribulose 5-phosphate bound complex showed no significant conformational change of the acidic loop. In both the *M. jannaschii* as well as in the *M. grisea* structure two different conformations of this loop, an open and a closed conformation, are observed. In the

ligand-free structures this loop points away from the active site cavity while it closes up this cavity and directly interacts with the metals in the complexes *via* the strictly conserved Glu26 (*M. jannaschii*) and Glu37 (*M. grisea*), respectively. In *C. albicans* this loop shows a conformation which is not compatible with any of the conformations mentioned above for the *M. jannaschii* and the *M. grisea* structures. As this loop points away from the active site we designate this conformation which is observed in the ligand-free form as well as in the complex as open and suggest that the closed conformation is a consequence of the metal-binding as observed for the *M. jannaschii* and *M. grisea* structures. The second loop (flap II) around residues 78–83 is also observed in a closed and an open conformation for the complexes and the ligand-free enzymes of *M. jannaschii* and *M. grisea*. In contrast to the *C. albicans* structure where this region is undefined by electron density in the ligand-free form as well as in the Ru5P-complex, in *M. jannaschii*, an insertion of 16 residues which occurs only in archaeal DHBPS (Figure 6), is part of this loop.

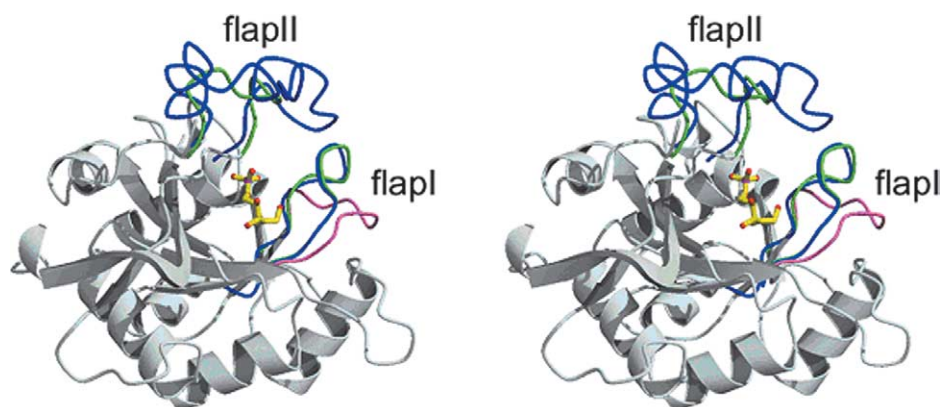


Figure 10. Overlay of the complex structures of 3,4-dihydroxy-2-butanone 4-phosphate synthases of *C. albicans*, *M. jannaschii* and *M. grisea*. *M. jannaschii*, blue; *M. grisea*, green; *C. albicans*, grey. The acidic loop of *C. albicans* DHBPS is highlighted in pink. Only the substrate Ru5P of the *C. albicans* complex is shown (yellow).

Conclusion

Flavocoenzymes appear to be absolutely indispensable in all organisms. Animals and certain microorganisms depend on the uptake of riboflavin as a vitamin. The endogenous production is absolutely essential at least in Gram-negative bacterial pathogens and probably in pathogenic yeast, which are virtually unable to acquire riboflavin from the environment due to the lack of an uptake system. Hence, inhibitors of riboflavin biosynthetic enzymes might be used as antibiotic agents directed against those microorganisms. Thus, the structure of the 3,4-dihydroxy-2-butanone 4-phosphate synthase of *C. albicans* in combination with biochemical data might be very helpful for the rational design of anti-infective agents. Immunosuppressed patients who are suffering from AIDS infections or having an organ transplantation would benefit from drugs that fight this organism.

Materials and Methods

Materials

5-Amino-6-ribitylamino-2,4-(1*H*,3*H*)-pyrimidinedione was synthesized according to published procedures.³⁵ 6,7-Dimethyl-8-ribityllumazine synthase was prepared as described earlier.³⁶ Ribose 5-phosphate, ribulose 5-phosphate and phosphoriboisomerase from spinach were from Sigma. Restriction enzymes and T4 DNA ligase were from New England Biolabs. EXT DNA Polymerase and Taq polymerase were from Finnzymes (Espoo, Finland). Oligonucleotides were synthesized by Thermo Electron GmbH (Ulm, Germany). DNA fragments were purified with the CP-Kit, Gel Extraction Kit or Miniprep Kits from Peqlab (Erlangen, Germany). Genomic DNA of *C. albicans* was obtained from the American type culture collection (ATCC No. 10231D).

Strains and plasmids

Bacterial strains and plasmids used in this study are summarized in Table 4. Transformation of *E. coli* was performed according to published procedures.³⁷ Unless otherwise stated, bacteria were grown at 37 °C in LB medium containing 170 mg μl⁻¹ ampicillin and 15 mg μl⁻¹ kanamycin where appropriate.

Construction of expression plasmids

C. albicans genomic DNA was used as template for PCR amplification with the primers CAR3-WT-Rbs-EcoRI (5' ataatagaattcattaagaggagaaattaactatgactaacatcttactctatt gaag 3') and CAR3-WT-BamHI-Hi (5' tattatggatccttattta gaaatatattcaactaattgg 3'). The resulting DNA fragment was restricted with the endonucleases EcoRI and BamHI and ligated into the equally treated vector pNCO113. The resulting plasmid was designated pNCO-CARib3-WT.

Gene synthesis

The partially complementary oligonucleotides CA-Rib3-1 and CA-Rib3-2 were annealed and treated with DNA polymerase (Figure 3). The resulting 110 bp segment was elongated by a series of six PCR amplifications using pairwise combinations of oligonucleotides according to Figure 3, the first cycle being performed with the oligonucleotides CA-Rib3-3 and CA-Rib3-4. The resulting 661 bp DNA fragment was treated with EcoRI and HindIII and was ligated into the plasmid pNCO113 which had been treated with the same restriction endonucleases. The ligation mixture was transformed into *E. coli* strain XL1-Blue affording the recombinant strain XL1 pNCO-CARib3-syn (Table 4).

Site-directed mutagenesis

Site-directed mutagenesis was performed using a PCR standard protocol as described elsewhere.³⁸ For the verification of mutations, oligonucleotides were designed to introduce recognition sites for specific endonucleases. All of the sequences were deposited in the GenBank sequence data base (Table 2).

Bacterial culture

Hyperexpression plasmids used in this study were expressed in *E. coli* strain XL1, with the exception of pNCO-CARib3-D92A which was expressed in *E. coli* strain M15 [pRep4]. XL1-cultures were grown at 37 °C with shaking for 24 hours. M15 [pRep4] pNCO-CARib3-D92A was cultured at 37 °C with shaking to an absorbance of $A_{600\text{ nm}}$. The suspension was cooled to 20 °C, β-D-isopropylthiogalactoside was added to a final concentration of 1 mM, and incubation was continued overnight. The cells were harvested by centrifugation, washed with 0.9% NaCl and stored at -20 °C.

Table 4. Bacterial strains and plasmids used in this study

| Designation | Relevant characteristics | Source |
|------------------------|---|------------|
| <i>E. coli</i> strains | | |
| XL1-Blue | recA1, endA1, gyrA96, thi-1, hsdR17, supE44, relA1, lac[F', proAB, lacI ^q ΔM15, Tn10(tet ^r)] | 56 |
| M15[pREP4] | lac, ara, gal, mtl, recA ⁺ , uvr ⁺ , Str ^R , (pREP4: Kan ^R , lacI) | 57 |
| Expression plasmids | <i>E. coli</i> expression vector | 57 |
| pNCO113 | | |
| pNCO-CARib3-WT | RIB3 gene genomic nucleotide sequence | This study |
| pNCO-CARib3-syn | RIB3 gene with optimized codon usage for <i>E. coli</i> | This study |
| pNCO-CARib3-C59A | RIB3 gene C59A mutant | This study |
| pNCO-CARib3-Y87A | RIB3 gene Y87A mutant | This study |
| pNCO-CARib3-D92A | RIB3 gene D92A mutant | This study |
| pNCO-CARib3-E166A | RIB3 gene E166A mutant | This study |

Protein purification

The cell pellet was suspended in 30 mM potassium phosphate (pH 7.0) containing 2 mM DTT. The suspension was ultrasonically treated and centrifuged (26,000g, 20 minutes). The supernatant was mixed with an equal volume of ice-cold saturated ammonium sulfate solution. The mixture was stirred on ice for 15 minutes and was then centrifuged. The supernatant was placed on a column of Phenyl Sepharose (20 ml) which had been equilibrated with 30 mM potassium phosphate (pH 7.0) containing 2 mM DTT and 2 M ammonium sulfate. The column was developed with 30 mM potassium phosphate (pH 7.0) containing 2 mM DTT. Fractions were combined, concentrated by ultrafiltration and placed on a Superdex 75 26/60 column. Elution was performed with 50 mM Tris hydrochloride (pH 7.5) containing 150 mM NaCl. Fractions were combined and concentrated by ultrafiltration.

Enzyme assay

Assay mixtures (100 μ l) contained 50 mM Tris hydrochloride (pH 7.5) 10 mM MgCl₂, 0.75 mM 5-amino-6-ribitylamino-2,4(1*H*,3*H*)-pyrimidinedione and 3,4-dihydroxy-2-butanone 4-phosphate synthase. The reaction was started by the addition of 100 μ l of 50 mM Tris hydrochloride (pH 7.5) containing 10 mM MgCl₂, 10 mM ribose 5-phosphate, 50 μ g of 6,7-dimethyl-8-ribityllumazine synthase of *E. coli*, and 1.25 units of phosphoriboisomerase which had been incubated for five minutes at 37 °C in order to generate ribulose 5-phosphate. The reaction was monitored photometrically at 410 nm.³³

Analytical ultracentrifugation

Experiments were performed with an analytical ultracentrifuge Optima XL-A from Beckman Instruments (Palo Alto, CA) equipped with absorbance optics. Aluminum double sector cells equipped with quartz windows were used throughout. The partial specific volume was estimated from the amino acid composition^{39,40} yielding a value of 0.733 ml g⁻¹.

Sedimentation equilibrium experiments were performed with 50 mM Tris hydrochloride (pH 7.5) containing 300 mM potassium chloride and 1.0 mg of protein per ml at 13,000 rpm and 4 °C.

Boundary sedimentation experiments were performed with a solution containing 50 mM Tris hydrochloride (pH 7.5) containing 300 mM potassium chloride and 2.9 mg of protein per ml at 59,000 rpm and 20 °C.

Circular dichroism spectroscopy

Measurements of circular dichroism were performed with a JASCO J-715 spectropolarimeter.

Crystallization

Crystallization was performed by the sitting drop vapour diffusion method. Droplets (3 μ l) containing 50 mM of Tris hydrochloride (pH 7.5) and 17–34 mg of protein per ml were mixed with 1 μ l of 85 mM sodium citrate (pH 5.0) containing 17% PEG 8000, and left to equilibrate over 300 μ l of the same solution. Co-crystallisation experiments with EDTA were carried out by mixing wild-type enzyme with 5 mM EDTA. Sitting drops were set up from 3 μ l of the complex solution

mixed with 1 μ l of 90 mM Mes/NaOH (pH 6.0) containing 18% PEG 8000. Soaking experiments with EDTA co-crystals were carried out with 2 mM D-ribose 5-phosphate for five minutes at 20 °C.

Data collection, data processing and phasing

All X-ray data were collected on a MARResearch345 image plate detector mounted on a Rigaku RU-200 rotating anode operated at 50 mM and 100 kV with λ (Cu K α)=1.542 Å. All data sets were collected under cryogenic conditions at 100 K using an Oxford cryostream. Prior to data collection, crystals were transferred into a buffer that contained 17.5% glycerol in addition to the components of the precipitating buffer. Diffraction intensities were integrated using the program DENZO and were scaled and merged using the HKL suite.⁴¹ The electron density was improved by solvent flattening using the program DM.

The structures were solved by molecular replacement using the program AMORE⁴² with the structure of the *E. coli* 3,4-dihydroxy-2-butanone 4-phosphate synthase³² (PDB-ID: 1G57) for the ligand-free DHBPS as Patterson search model. Table 3 gives a summary of the data collection and phasing statistics.

Model building and refinement

The 1.6 Å (native) and 1.7 Å (Ru5P) electron density maps were of sufficient quality to permit unambiguous chain tracing for about 90% of the model in the first round of model building using the program MAIN.⁴³ Refinement steps involved conjugate minimization, simulated annealing, and B-factor refinement with the program CNS using the mlf target.⁴⁴ For cross-validation, a random test set of 5% of the total number of reflections was excluded from the refinement and used for the calculation of the free R-factor.⁴⁵ The refinement was carried out on the resulting model until convergence was reached at an R-factor of 19.7% (native) and 18.4% (Ru5P) and an R_{free} of 22.8% (native) and 21.8% (Ru5P). The crystallographic refinements were carried out at 1.6 Å (native) and 1.7 Å (Ru5P).

The Ramachandran plot⁴⁶ calculated with the program PROCHECK⁴⁷ showed no residues with angular values in forbidden areas; 88.9% (native) and 89.9% (Ru5P) of the non-glycine residues are in the most favored regions, and 11.1% (native) and 10.1% (Ru5P) are in additionally allowed regions.

Analysis and graphical representation

Stereochemical parameters were assessed throughout refinement with PROCHECK.⁴⁷ Secondary structure elements were assigned with STRIDE.⁴⁸ Structural Figures were prepared with MOLSCRIPT,⁴⁹ BOBSCRIPT,⁵⁰ ALSRIPT⁵¹ and Swiss-PDB Viewer†.

Miscellaneous

DNA was sequenced using the Sanger method⁵² by the custom sequencing service of GATC Biotech (Konstanz, Germany). N-terminal protein sequencing was performed according to the automated Edman method using a 471A Protein Sequencer (Perkin-Elmer). Protein concentration was determined by published

† <http://www.expasy.ch/spdv>

procedures.⁵³ Electrospray mass spectrometry experiments were performed as described by Mann and Wilm⁵⁴ using a triple quadrupole ion spray mass spectrometer API365 (SciEx, Thornhill, ON, Canada). SDS polyacrylamide gel electrophoresis using 16% polyacrylamide gels was performed as described by Laemmli with molecular mass standards provided by Sigma.⁵⁵

Protein Data Bank accession numbers

The coordinates have been deposited in the Protein Data Bank (accession codes 1TKS, 1TKU) and will be released upon publication.

Acknowledgements

We thank Rebecca Blom, Sebastian Schwamb and Thomas Wojtulewicz for skillful technical assistance. We are grateful to Gerald Richter for help in analytical ultracentrifugation. This work was supported by the Fonds der Chemischen Industrie and the Hans-Fischer-Gesellschaft e.V.

References

- Bacher, A. (1991). Biosynthesis of flavins. In *Chemistry and Biochemistry of Flavoenzymes* (Müller, F., ed.) vol. 1, pp. 215–259, CRC Press Boca Raton, FL.
- Briggs, W. R. & Huala, E. (1999). Blue-light photoreceptors in higher plants. *Annu. Rev. Cell Dev. Biol.* **15**, 33–62.
- Salomon, M., Eisenreich, W., Durr, H., Schleicher, E., Knieb, E. Massey, V. *et al.* (2001). An optomechanical transducer in the blue light receptor phototropin from *Avena sativa*. *Proc. Natl Acad. Sci. USA*, **98**, 12357–12361.
- Meighen, E. A. (1991). Molecular biology of bacterial bioluminescence. *Microbiol. Rev.* **55**, 123–142.
- Meighen, E. A. (1993). Bacterial bioluminescence: organization, regulation, and application of the lux genes. *FASEB J.* **7**, 1016–1022.
- O’Kane, D. J. & Prasher, D. C. (1992). Evolutionary origins of bacterial bioluminescence. *Mol. Microbiol.* **6**, 443–449.
- Thompson, C. I. & Sancar, A. (2002). Photolyase/cryptochrome blue-light photoreceptors use photon energy to repair DNA and reset the circadian clock. *Oncogene*, **21**, 9043–9056.
- Young, D. W. (1986). The biosynthesis of the vitamins thiamin, riboflavin, and folic acid. *Nature Prod. Rep.* **3**, 395–419.
- Bacher, A., Eberhardt, S., & Richter, G. (1996). Biosynthesis of riboflavin. In *Escherichia and Salmonella* (Neidhardt, F. C., Ingraham, J. L., Low, K. B., Magasanik, B., Schaechter, M. & Umberger, H. E., eds), vol. 1, American Society for Microbiology, Washington, DC.
- Bacher, A., Eberhardt, S., Eisenreich, W., Fischer, M., Herz, S. Illarionov, B. *et al.* (2001). Biosynthesis of riboflavin. *Vitam. Horm.* **61**, 1–49.
- Hollander, I. & Brown, G. M. (1979). Biosynthesis of riboflavin: reductase and deaminase of *Ashbya gossypii*. *Biochem. Biophys. Res. Commun.* **89**, 759–763.
- Foor, F. & Brown, G. M. (1975). Purification and properties of guanosine triphosphate cyclohydrolase II from *Escherichia coli*. *J. Biol. Chem.* **250**, 3545–3551.
- Burrows, R. B. & Brown, G. M. (1978). Presence in *Escherichia coli* of a deaminase and a reductase involved in biosynthesis of riboflavin. *J. Bacteriol.* **136**, 657–667.
- Nielsen, P. & Bacher, A. (1981). Biosynthesis of riboflavin. Characterization of the product of the deaminase. *Biochim. Biophys. A*, **662**, 312–317.
- Richter, G., Fischer, M., Krieger, C., Eberhardt, S., Lüttgen, H., Gerstenschläger, I. & Bacher, A. (1997). Biosynthesis of riboflavin. Characterization of the bifunctional deaminase/reductase of *Escherichia coli* and *Bacillus subtilis*. *J. Bacteriol.* **179**, 2022–2028.
- Richter, G., Ritz, H., Katzenmeier, G., Volk, R., Kohnle, A. Lottspeich, F. *et al.* (1993). Biosynthesis of riboflavin: cloning, sequencing, mapping and expression of the gene coding for GTP cyclohydrolase II in *E. coli*. *J. Bacteriol.* **175**, 4045–4051.
- Neuberger, G. & Bacher, A. (1986). Biosynthesis of riboflavin. Enzymatic formation of 6,7-dimethyl-8-ribityllumazine by heavy riboflavin synthase from *Bacillus subtilis*. *Biochem. Biophys. Res. Commun.* **139**, 1111–1116.
- Kis, K. & Bacher, A. (1995). Substrate channeling in the lumazine synthase/riboflavin synthase complex of *Bacillus subtilis*. *J. Biol. Chem.* **270**, 16788–16795.
- Kis, K., Volk, R. & Bacher, A. (1995). Biosynthesis of riboflavin. Studies on the reaction mechanism of 6,7-dimethyl-8-ribityllumazine synthase. *Biochemistry*, **34**, 2883–2892.
- Plaut, G. W., Beach, R. L. & Aogaichi, T. (1970). Studies on the mechanism of elimination of protons from the methyl groups of 6,7-dimethyl-8-ribityllumazine by riboflavin synthetase. *Biochemistry*, **9**, 771–785.
- Plaut, G. W. E. (1960). Studies on the stoichiometry of the enzymatic conversion of 6,7 dimethyl-8-ribityllumazine to riboflavin. *J. Biol. Chem.* **235**, 41–42.
- Plaut, G. W. E. (1963). Studies on the nature of the enzymatic conversion of 6,7-dimethyl-8-ribityllumazine to riboflavin. *J. Biol. Chem.* **238**, 2225–2243.
- Plaut, G. W. E. & Harvey, R. A. (1971). The enzymatic synthesis of riboflavin. *Methods Enzymol.* **18**, 515–538.
- Volk, R. & Bacher, A. (1990). Studies on the 4-carbon precursor in the biosynthesis of riboflavin. *J. Biol. Chem.* **265**, 19479–19485.
- Steinbacher, S., Schiffmann, S., Richter, G., Huber, R., Bacher, A. & Fischer, M. (2003). Structure of 3,4-dihydroxy-2-butanone 4-phosphate synthase from *Methanococcus jannaschii* in complex with divalent metal ions and the substrate ribulose 5-phosphate. *J. Biol. Chem.* **278**, 42256–42265.
- Steinbacher, S., Schiffmann, S., Huber, R., Bacher, A. & Fischer, M. (2004). Metal sites in 3,4-dihydroxy-2-butanone 4-phosphate synthase from *Methanococcus jannaschii* in complex with the substrate ribulose 5-phosphate. *Acta Crystallog. sect. D*, **60**, 1338–1340.
- Shavlovsky, G. M., Teslyar, G. E. & Strugovshchikova, L. P. (1982). Regulation of flavogenesis in riboflavin-dependent *Escherichia coli* mutants. *Mikrobiologiya*, **51**, 986–992.
- Shavlovsky, G. M., Sibirny, A. A., Kshanovskaya, B. V., Koltun, L. V. & Logvinenko, E. M. (1979). Genetic classification of riboflavinless mutants of *Pichia guilliermondii* yeast. *Soviet Genet.* **15**, 1561–1568.
- Oltmanns, O., Bacher, A., Lingens, F. & Zimmermann,

- F. K. (1969). Biochemical and genetic classification of riboflavine deficient mutants of *Saccharomyces cerevisiae*. *Mol. Gen. Genet.* **105**, 306–313.
30. Liao, D.-I., Zheng, Y.-J., Viitanen, P. V. & Jordan, D. B. (2002). Structural definition of the active site and catalytic mechanism of 3,4-dihydroxy-2-butanone 4-phosphate synthase. *Biochemistry*, **41**, 1795–1806.
31. Richter, G., Kelly, M., Krieger, C., Yu, Y., Bermel, W., Karlsson, G. *et al.* (1999). NMR studies on the 46-kDa dimeric protein, 3,4-dihydroxy-2-butanone 4-phosphate synthase, using ²H, ¹³C, and ¹⁵N-labelling. *Eur. J. Biochem.* **261**, 57–65.
32. Liao, D.-I., Calabrese, J. C., Wawrzak, Z., Viitanen, P. V. & Jordan, D. B. (2001). Crystal structure of 3,4-dihydroxy-2-butanone 4-phosphate synthase of riboflavin biosynthesis. *Structure*, **9**, 11–18.
33. Fischer, M., Römisch, W., Schiffmann, S., Kelly, M., Oschkinat, H., Steinbacher, S. *et al.* (2002). Biosynthesis of riboflavin in archaea studies on the mechanism of 3,4-dihydroxy-2-butanone 4-phosphate synthase of *Methanococcus jannaschii*. *J. Biol. Chem.* **277**, 41410–41416.
34. Liao, D.-I., Viitanen, P. V. & Jordan, D. B. (2000). Cloning, expression, purification and crystallization of dihydroxybutanone phosphate synthase from *Magnaporthe grisea*. *Acta Crystallog. sect. D*, **56**, 1495–1497.
35. Bacher, A. (1986). Heavy riboflavin synthase from *Bacillus subtilis*. *Methods Enzymol.* **122**, 192–199.
36. Moertl, S., Fischer, M., Richter, G., Tack, J., Weinkauff, S. & Bacher, A. (1996). Biosynthesis of riboflavin. Lumazine synthase of *Escherichia coli*. *J. Biol. Chem.* **271**, 33201–33207.
37. Hanahan, D. (1983). Studies on transformation of *Escherichia coli* with plasmids. *J. Mol. Biol.* **166**, 557–580.
38. Fischer, M., Haase, I., Kis, K., Meining, W., Ladenstein, R., Cushman, M. *et al.* (2003). Enzyme catalysis via control of activation entropy: site-directed mutagenesis of 6,7-dimethyl-8-ribityl-lumazine synthase. *J. Mol. Biol.* **326**, 783–793.
39. Cohn, E. J. & Edsall, J. T. (1943). Proteins, amino acids and peptides as ions and dipolar ions. *Am. Chem. Soc. Monograph*, No. 90. Reinhold: New York.
40. Laue, T. M., Shah, B. D., Ridgeway, T. M. & Pelletier, S. L. (1992). Computer-aided interpretation of analytical sedimentation data for proteins. In *Analytical Ultracentrifugation in Biochemistry and Polymer Science* (Harding, S. E., Rowe, A. J. & Horton, J. C., eds), Royal Society of Chemistry, Cambridge.
41. Ottwinowski, Z. & Minor, W. (1997). Proceedings of X-ray diffraction data collected in oscillations mode. *Methods Enzymol.* **276**, 307–326.
42. Navaza, J. (1994). AMoRE: an automated package for molecular replacement. *Acta Crystallog. sect. A*, **50**, 157–163.
43. Turk, D. (1992). Weiterentwicklung eines Programmes für Molekülgraphik und Elektronendichte-Manipulation und seine Anwendung auf verschiedene Protein-Strukturaufklärungen. PhD, Technische Universität.
44. Bruenger, A. T. (1998). Crystallography and NMR system: a new software suite for macromolecular structure determination. *Acta Crystallog. sect. D*, **54**, 905–921.
45. Bruenger, A. (1992). Free R value: a novel statistical quantity for assessing the accuracy of crystal structures. *Nature*, **355**, 472–475.
46. Ramachandran, G. N. & Sasisekharan, V. (1968). Conformation of polypeptides and proteins. *Advan. Protein Chem.* **23**, 283–437.
47. Laskowski, R. A., McArthur, M. W., Moss, D. S. & Thornton, J. M. (1993). PROCHECK—a program to check the stereochemical quality of protein structures. *J. Appl. Crystallog.* **26**, 283–291.
48. Frishman, D. & Argos, P. (1995). Knowledge-based protein secondary structure assignment. *Proteins: Struct. Funct. Genet.* **23**, 566–579.
49. Kraulis, P. J. (1991). MOLSCRIPT: a program to produce both detailed and schematic plots of protein structures. *J. Appl. Crystallog.* **24**, 946–950.
50. Esnouf, R. M. (1997). An extensively modified version of MolScript that includes greatly enhanced coloring capabilities. *J. Mol. Graph Model.* **15**, 132–134.
51. Barton, G. J. (1993). ALSRIPT a tool to format multiple sequences alignments. *Protein Eng.* **6**, 37–40.
52. Sanger, F., Niklen, S. & Coulson, A. R. (1977). DNA sequencing with chain-terminating inhibitors. *Proc. Natl Acad. Sci. USA*, **74**, 5463–5467.
53. Bradford, M. M. (1976). A rapid and sensitive method for the quantitation of microgram quantities of protein utilizing the principle of protein-dye binding. *Anal. Biochem.* **72**, 248–254.
54. Mann, M. & Wilm, M. (1995). Electrospray mass spectrometry for protein characterization. *Trends Biochem. Sci.* **20**, 219–224.
55. Laemmli, U. K. (1970). Cleavage of structural proteins during the assembly of the head of bacteriophage T4. *Nature*, **227**, 680–685.
56. Bullock, W. O., Fernandez, J. M. & Short, J. M. (1987). XL-blue: a high efficiency plasmid transforming *recA* *Escherichia coli* strain with β -galactosidase selection. *BioTechniques*, **5**, 376–379.
57. Stueber, D., Matile, H. & Garotta, G. (1990). System for high level production in *E. coli* and rapid purification of recombinant proteins: application to epitope mapping, preparation of antibodies and structure function analysis. In *Immunological Methods IV* (Lefkovits, I & Pernis, P., eds).

Edited by I. Wilson

(Received 24 March 2004; received in revised form 15 June 2004; accepted 15 June 2004)